Journal of AI and Data Mining
Vol 5, No 1, 2017, 89-100

DOI: 10.22044/jadm.2016.655

Using a new modified harmony search algorithm to solve multi-objective reactive power dispatch in deterministic and stochastic models

Kh. Valipour* and A. Ghasemi

Technical Engineering Department, University of Mohaghegh Ardabili, Ardabil, Iran.

Received 12 January 2016; Accepted 30 May 2016
*Corresponding author: kh_valipour@uma.ac.ir (Kh. Valipour.)

Abstract

The optimal reactive power dispatch (ORPD) problem is a very important aspect in power system planning, and it is a highly non-linear, non-convex optimization problem because it consists of both the continuous and discrete control variables. Since a power system has an inherent uncertainty, this paper presents both the deterministic and stochastic models for the ORPD problem in multi-objective and single-objective formulations, respectively. The deterministic model considers three main issues in the ORPD problem including the real power loss, voltage deviation, and voltage stability index. However, in the stochastic model, the uncertainties in the demand and equivalent availability of shunt reactive power compensators have been investigated. To solve them, we proposed a new modified harmony search algorithm (HSA), implemented in single and multi-objective forms. Since, like many other general purpose optimization methods, the original HSA often traps into the local optima, an efficient local search method called chaotic local search (CLS) and a global search operator are proposed in the internal architecture of the original HSA algorithm to improve its ability in finding the best solution because the ORPD problem is very complex, with different types of continuous and discrete constrains, i.e. excitation settings of generators, sizes of fixed capacitors, tap positions of tap changing transformers, and amount of reactive compensation devices. Moreover, the fuzzy decision-making method is employed to select the best solution from the set of Pareto solutions. The proposed model is individually examined and applied on different test systems. The simulation results show that the proposed algorithm is suitable and effective for the reactive power dispatch problem compared to the other available algorithms.

Keywords: *Reactive Power Dispatch, Modified HSA, Multi-objective, System Stability, Stochastic Model.*

1. Introduction

The optimal reactive power dispatch (ORPD) problem can be divided into two parts, known as the real and reactive power dispatch problems. The real power dispatch problem aims to minimize the total cost of real power generation from thermal power plants at various stations [1]. However, reactive power dispatch controls the power system stability and power quality, i.e. voltage stability and power loss. Generally, the objective of ORPD is to minimize the real power loss and increase the voltage stability in the power system, while satisfying various discrete and continues constraints [2].

Recently, many scientific papers have been dedicated to the ORPD problem, which can be classified into two groups, classical and intelligent computing methods. Classical computing methods consist of some well-known mathematical strategies such as linear programming (LP) [3], non-linear programming (NLP) [4], quadratic programming [5], and decomposition technique [6]. This group is computationally fast but they have several limitations like (i) the need for continuous and differentiable objective functions, (ii) easy convergence to local minima. and (iii) difficulty in handling a very large number of variables. Therefore, it is vital to develop some intelligent methods that are capable of overcoming these shortages. In another group, computational intelligence-based techniques have been proposed for the application of reactive power optimization. In [7], a new modified version of honey bee mating optimization called the parallel vector evaluated honey bee mating optimization (PVEHBMO) based on multi-objective formulation has been proposed to solve the RPD problem. In [8], the authors have presented a quasi-oppositional differential evolution to solve the ORPD problem of a power system. In [9], the authors have proposed a multi-objective differential evolution (MODE) to solve the multi-objective optimal reactive power dispatch (MORPD) problem by minimizing the active power transmission loss and voltage deviation, and maximizing the voltage stability, while varying the control variables such as the generator terminal voltages, transformer taps, and reactive power output of shunt compensators. Pareto-efficient 12-h variable double auction bilateral power transactions have been considered in [10]. The effect of that on the economic welfare has been observed, while solving the reactive power dispatch (RPD) by differential evolution using the random localization technique. This has been accomplished by a combination of static and dynamic var compensators. Out of these 12-h variable power transactions, the Pareto-efficient transactions, which are reconciled by planed biding, have provided the maximum global welfare. In [11], the authors have presented a new meta-heuristic method, namely gray wolf optimizer (GWO), which is inspired from gray wolves'leadership and hunting behaviors to solve the optimal reactive power dispatch (ORPD) problem.

The aforementioned papers show that the optimization methods have a good potential to solve the ORPD problem. The ORPD with high optimal variables and constrains requires a more effective method to avoid the local optimal solutions, and it has well-distribution of non-dominated solutions, while satisfying the diversity characteristics. A new meta-heuristic algorithm, mimicking the improvisation process of music players, has been recently developed and named the harmony search algorithm (HSA) [12]. Due to its many positive features, being simple in concept and easy to implement, flexibility, the possibility of using chaotic maps and of developing hybrids from combinations with other techniques, the HSA algorithm has been successfully applied to the optimization of complex mathematical functions with or without constraints [13]. Unfortunately, the standard HSA often converges to local optima. In order to improve the fine-tuning characteristic of HSA, an improved HSA has been proposed, enhancing the fine-tuning characteristic and convergence rate of harmony search [14-15]. This paper proposes two modifications in the local and global operators. In the local term, a new CLS operator is presented to update each particle in the search space. In the global part, the pitch adjusting rate (PAR) and the distance bandwidth (bw) are rewritten, which are important coefficients in exploration and exploitation. Moreover, HSA is developed as a stochastic optimization algorithm; it can find an optimal solution within a short calculation time. The results obtained from three test systems in the ORPD problem show that the proposed method has a robust convergence and makes an acceptable distribution in the Pareto-optimal solutions.

2. Deterministic formulation of ORPD problem

In this section, the deterministic formulation of the ORPD problem is presented.

2.1. Problem objectives

• *Objective 1: power-loss minimization*

Transmission losses are construed as a loss of revenue by the utility. The transmission loss can be expressed by [7]:

$$J_1 = \mathrm{P}_{loss}(x,u) = \sum_{k=1}^{N_L} g_k [V_i^2 + V_j^2 - 2V_i V_j \cos(\theta_i - \theta_j)) \quad (1)$$

where, g_k is the conductance of the line ***i-j***, V_i and V_j are the line voltages, and θ_i and θ_j are the line angles at the *i* and *j* line ends, respectively, *k* is the k^{th} network branch that connects bus i to bus j, i = 1, 2, . . . , *ND*, where *ND* is the set of numbers of power demand bus, and *j* = 1, 2, . . . , N_j, where N_j is the set of numbers of buses adjacent to bus *j*. PG is the active power in lines *i* and *j*. x and u are the vector of dependent variables and the vector of control variables, respectively.

• *Objective 2: Minimization of voltage deviation*

The aim of this function is to minimize the absolute voltage deviation of load bus voltages from their desired values:

$$J_2 = VD(x,u) = \sum_{i=1}^{Nd} |V_i - V_i^{sp}| \quad (2)$$

where, N_d is the number of load buses.

• *Objective 3: Minimization of L-index voltage stability*

It is a static voltage stability measure of power system, which is computed based on the normal load flow solution. *L-index* L_j of the j^{th} bus can be expressed by:

$$\begin{cases} L_j = \left| 1 - \sum_{i=1}^{N_{PV}} F_{ji} \dfrac{V_i}{V_j} \right|, \; j = 1,2,...,N_{PQ} \\ F_{ji} = -[Y_1]^{-1}[Y_2] \end{cases} \quad (3)$$

where, N_{PV} and N_{PQ} are the number of PV and PQ buses, respectively. Y_1 and Y_2 refer to the sub-matrices of the YBUS matrix one gets:

$$\begin{bmatrix} I_{PQ} \\ I_{PV} \end{bmatrix} = \begin{bmatrix} Y_1 & Y_2 \\ Y_3 & Y_4 \end{bmatrix} \begin{bmatrix} V_{PQ} \\ V_{PV} \end{bmatrix} \quad (4)$$

The L-index is calculated for all the PQ buses. L_j shows no load case and voltage collapse conditions of bus j in the range of (0, 1). Thus the objective function is represented by:

$$L = \max(L_j),\ j = 1,2,...,N_{PQ} \quad (5)$$

In the ORPD problem, an incorrect set of control variables may increase the value of L-index, and leads to a voltage instability. Let the maximum value of *L-index* be L_{max}. Therefore, to enhance the voltage stability, and to keep the system far from the voltage collapse margin, one gets:

$$J_3 = VL(x,u) = L_{\max} \quad (6)$$

2.2. Objective constraints

• *Constraints 1: Equality Constraints*

In the ORPD problem, the power generation must be equal to the sum of the demand (P_D) and the power loss in the transmission lines:

$$\begin{cases} P_{G_i} - P_{D_i} = V_i \sum_{j=1}^{N_B} V_j [G_{ij} \cos(\theta_i - \theta_j) + B_{ij} \sin(\theta_i - \theta_j)] \\ Q_{G_i} - Q_{D_i} = V_i \sum_{j=1}^{N_B} V_j [G_{ij} \sin(\theta_i - \theta_j) - B_{ij} \cos(\theta_i - \theta_j)] \end{cases} \quad (7)$$

where, NB is the number of buses; Q_{Gi} is the reactive power generated at the i^{th} bus; and P_{Di} and Q_{Di} are the i^{th} bus load real and reactive power, respectively; G_{ij} and B_{ij} are the transfer conductance and susceptance between bus i and bus j, respectively; V_i and V_j are the voltage magnitudes at bus i and bus j, respectively; and θ_i and θ_j are the voltage angles at bus i and bus j, respectively.

• *Constraints 2: Generation Capacity Constraints*

Generally, the generator outputs and bus voltage constrains by lower and upper limits are as follow:

$$Q_i^{\min} \le Q_i \le Q_i^{\max}, v_i^{\min} \le v_i \le v_i^{\max} \quad (8)$$

where, P_i^{min} and P_i^{max} are the minimum and maximum values, respectively.

• *Constraints 3: Line-flow constraints*

One of the main constrains in the ORPD problem is the maximum transfer capacity of the transmission line. These constrains can be calculated as follows:

$$\left| S_{Lf,k} \right| \le S_{Lf,k}^{\max},\ k = 1,2,...,L \quad (9)$$

where, $S_{Lf,k}$ is the real power flow of line k; $S_{Lf,k}^{\max}$ is the power flow upper limit of line k, and subscript L denotes the number of transmission lines.

• *Constraints 4: Transformer*

The transformer tap setting is restricted by its lower and upper values:

$$T_i^{\min} \le T_i \le T_i^{\max} \quad (10)$$

2.3. Problem formulation

As results, the proposed deterministic multi-objective ORPD problem can be formulated as:

$$\min_{x,u} [\underbrace{\mathrm{P}_{loss}(x,u)}_{J_1}, \underbrace{VD(x,u)}_{J_2}, \underbrace{VL(x,u)}_{J_3}]$$

$$\begin{aligned} &\textit{subject to}: \\ &g(x,u) = 0 \\ &h(x,u) \le 0 \\ &\textit{where}, \mathrm{x^T} = [[\mathrm{V_L}]^\mathrm{T}, [\mathrm{Q_G}]^\mathrm{T}, [\mathrm{S_L}]^\mathrm{T}], \\ &\mathrm{u^T} = [[\mathrm{V_G}]^\mathrm{T}, [\mathrm{T}]^\mathrm{T}, [\mathrm{Q_C}]^\mathrm{T}] \end{aligned} \quad (11)$$

where, g and h are the equality and inequality constraints, respectively; [V_L], [Q_G], and [S_L] are the vector of load bus voltages, generator reactive power outputs, and transmission line loadings, respectively; and [V_G], [T], and [Q_C] are the vector of generator bus voltages, transformer taps, and reactive compensation devices, respectively.

3. Stochastic formulation of ORPD problem

In practice, power injections, especially from intermittent renewable sources, and demand are of uncertainties [16-17]. To aim with this cope, in this section, the load uncertainty is developed in the stochastic form in the ORPD problem. Usually the probability distribution of a random variable is represented using a finite set of scenarios. In other words, each scenario (s^{th}) has an associated probability of occurrence (ξ_s). From (1), variable ψ can be defined as:

$$\psi = \sum_{n \in L} pL_n \quad (12)$$

The expected value for ψ can be given by:

$$E[\psi] = \sum_{s \in S} \xi_s . \psi_s = \sum_{s \in S} \xi_s . \left(\sum_{n \in TL} pL_n \right) = \sum_{s \in S} \sum_{n \in TL} \xi_s . pL_{n,s} \quad (13)$$

Substituting (12) and (13), one gets:

$$\min\{f(x) + E[\psi(y)]\} \quad (14)$$

Finally, the stochastic formulation of power loss can be calculated as follows:

$$\begin{aligned} &\min_{\substack{v,\delta,tab,q^{SH} \\ P_{slack},q_G}} f = \sum_{s \in S} \sum_{n \in TL} \xi_s . pL_{n,s} \\ &P_{p,s}^G + p_{slack,s}^G = P_{l,s}^D + P_{i,s}(v,\delta,tab) \\ &q_{j,s}^G = Q_{l,s}^D + Q_{i,s}(v,\delta,tab) + q_{k,s}^{SH} \\ &\underline{Q}_j^G \le q_{j,s}^G \le \overline{Q}_j^G,\ \underline{Q}_k^{SH} \le q_{k,s}^{SH} \le \overline{Q}_k^{SH},\ \underline{V}_i \le v_{i,s} \le \overline{V}_i \quad (15) \\ &\underline{Tap}_m \le tap_{m,s} \le \overline{Tap}_m,\ |s_{n,s}| \le \overline{S}_n \\ &\forall \{i \in B, k \in SH, p \in PV, j \in \{PV \cup slack\}, \\ &l \in PQ, m \in TAP, n \in TL, s \in S\} \end{aligned}$$

Constraints Eqs. (7)-(11) in the deterministic model are modified to take into account all the different scenarios of demand $s \in S$, such that modifications are shown in constraints Eq. (15) in the stochastic model.

4. Multi-objective MHSA

4.1. Standard HSA

In this section, the original HSA is briefly introduced; more details can be found in [12].

```
Start
Objective function f(x), x=(x1,x2, …,xd)^T
Generate initial harmonics (real number arrays)
Define pitch adjusting rate (PAR), pitch limits and bandwidth
Define harmony memory accepting rate (r_accept)
while t<Max number of iterations
    Generate new harmonics by accepting best harmonics
    Adjust pitch to get new solutions
      if (rand>r_accept), choose an existing harmonic randomly
      else if (rand>PAR), adjust the pitch randomly within limits
           else generate new harmonics via randomization
           end if
         Accept the new harmonics (solutions) if better
      end
Find the current best solutions
End
```

Figure 1. Pseudo-code of standard HSA.

This algorithm has three main components, as shown in figure 1. It is clear that the probability of randomization can be given by:

$$P_{random} = 1 - r_{accept} \tag{16}$$

and the actual probability of adjusting pitches is given by:

$$P_{pitch} = r_{accept} \times PAR \tag{17}$$

4.2. Modified HSA

This algorithm shows a good performance in an optimization problem, although the main shortage of the HSA algorithm comes from this fact that it may miss the optimum solution or converge to a near optimum solution. However, it has a flexible and well-balanced mechanism to enhance the global and local exploration abilities. Therefore, the following modifications are proposed.

- *Modification of bw and PAR*

Generally, the parameters PAR and *bw* are arbitrarily fixed. It is clear that they can affect the stochastic nature of HSA. Therefore, a time-varying operator is proposed to keep away from this difficulty:

$$PAR_i = PAR_{\min} + \frac{i}{H}(PAR_{\max} - PAR_{\min}) \tag{18}$$

$$bw_i = bw_{\max} \times \exp\left(i \times \frac{\ln\left(\frac{bw_{\min}}{bw_{\max}}\right)}{H}\right) \tag{19}$$

where, PAR_{min} and PAR_{max} are the minimum and maximum values for the pitch adjustment rate in the search space, respectively; and H and i are the maximum and current iterations, respectively.

• *Global searching operator*

In order to have an effective global search, combine the genetic operator as follows:

$$\begin{aligned}
&\textit{for}\ \ \text{i=1:N}\\
&\quad penalty_i = abs(x_i^{best} - x_i^{worst});\\
&\quad x_i^{New} = x_i^{best} \pm penalty_i;\\
&\quad \textit{if}\ \ \text{rand} \le \text{T}\\
&\qquad x_i^{New} = x_i^{\min} + \text{rand} \times (x_i^{\max} - x_i^{\min});\\
&\quad \textit{end}\\
&\textit{end}
\end{aligned} \tag{20}$$

The superscripts *best* and *worst* refer to the global best and worst solutions for variable *x*, respectively. The parameter *penalty* is the guarantee for the global search ability. In other words, after some evaluations, HSA may reach a local solution and *penalty* goes to zero, and hereby, the algorithm will be stagnated. To avoid this shortage, generate some random harmonies, and replace the worse harmonies. The number of new random harmonies depends on the problem and size of HM. The new random harmonies increase the *penalty* parameter, and lead to new exploration in finding a better solution.

• *Local searching operator (CLS)*

Chaos is a random-like process found in a non-linear, dynamical system, which is non-period, non-converging, and bounded [17]. The proposed CLS-integrated HSA can be formulated as follows:

$$c_{i+1}^j = \begin{cases} 2c_i^j, if\ \ 0 < c_i^j \le 0.5 \\ 2(1-c_i^j), if\ \ 0.5 < c_i^j \le 1 \end{cases}, j = 1,2,...,Ng \tag{21}$$

where, C_{i+1}^j is the j^{th} chaotic variable of i^{th} iteration. This combination can be summarized as follows:

i) Generate an initial population:

$$\begin{aligned}
&X_{cls}^0 = [X_{cls,0}^1, X_{cls,0}^2, ..., X_{cls,0}^{Ng}]_{1\times N_g}\\
&cx_0 = [cx_0^1, cx_0^2, ..., cx_0^{Ng}]\\
&cx_0^j = \frac{X_{cls,0}^j - P_{j,\min}}{P_{j,\max} - P_{j,\min}}, j = 1,2,...,Ng
\end{aligned} \tag{22}$$

where, the chaos variable can be obtained by:

$$\begin{aligned}
&x_{cls}^i = [x_{cls,i}^1, x_{cls,i}^2, ..., x_{cls,i}^{Ng}]_{1\times N_g}, i = 1,2,...,N_{chaos}\\
&x_{cls,i}^j = cx_{i-1}^j \times (P_{j,\max} - P_{j,\min}) + P_{j,\min}, j = 1,2,...,N_g
\end{aligned} \tag{23}$$

ii) Measure the chaotic variables:

$$cx_i = [cx_i^1, cx_i^2, ..., cx_i^{Ng}], i = 0,1,2,...,N_{choas}$$
$$cx_{i+1}^j = base\ CLS \quad j = 1,2,...,Ng \tag{24}$$
$$cx_0^j = rand(0)$$

where, N_{chaos} is the number of individuals for CLS; cx_i^{Ng} is the i^{th} chaotic variable; *rand()* is a random number at the range (0,1); *Ng* is the number of units; and X^i_{cls} is the current position of the harmony-based chaos theory.

iii): Map the decision variables

iv): Convert the chaotic variables to the decision variables

v): Evaluate the new solution with decision variables.

4.3. Non-dominated sort and crowding distance

In this process, the entire population is sorted with its non-dominated level. Each solution is assigned with a fitness value. Perform the non-dominated sort method on the initial population, and calculate the rank: $rank_1$, $rank_2$, $rank_3$...., etc. After the non-dominated sort is done, the crowding distance is assigned to each solution. The crowding distance is assigned front wise. Compare the crowding distance between two individuals in different fronts [9, 10]. Hereby, the density of the surrounding individuals of i is expressed by i_d, which is the smallest range that contains i but does not contain other points around the individual i. This process can be expressed as follows:

i) For each front F_i, l is the number of individual, i.e. $|F_i| = l$.

ii) For every individual i, set the initial crowding distance $i_d = 0$.

iii) Set $1_d = l_d = \infty$. For each individual i, $P[i].k$ denotes the value for the k^{th} objective function.

iv) Let i cycle be from 2 to $l-1$, and calculate the following expression to define the crowding distance for each individual

$$i_d = i_d + \sum_{k=1}^{m}\left(\frac{(P[i+1].f_k - P[i-1].f_k)}{f_k^{\max} - f_k^{\min}} \right) \tag{25}$$

The graphical outlook for non-dominated sort and crowding distance is shown in figure 2.

4.4. Best compromise solution

Fuzzy decision-maker is one of the multi-criteria decision methods that provide the best decision between a set of solutions. It can help the designer to make the best decisions that are consistent with their values, goals, and performances [17]. Hereby, firstly, the solution is assigned with the following triangular membership function:

$$\mu_i = \frac{f_i^{\max} - f_i}{f_i^{\max} - f_i^{\min}} \tag{26}$$

$$FDM_i = \begin{cases} 0 & \mu_i \le 0 \\ \mu_i & 0 < \mu_i < 1 \\ 1 & \mu_i \ge 1 \end{cases} \tag{27}$$

where, f^i_{min} and f^i_{max} are the maximum and minimum values for the i^{th} function response of the selected k^{th} solution, respectively. The normalized membership function FDM^k can be calculated by:

$$FDM^k = \left[\frac{\sum_{i=1}^{N_{obj}} FDM_i^k}{\sum_{j=1}^{M}\sum_{i=1}^{N_{obj}} FDM_i^j} \right] \tag{28}$$

where, M is the number of non-dominated solutions, and Nob_j is the number of objective functions. Figure 3 illustrates a typical shape of the employed membership function.

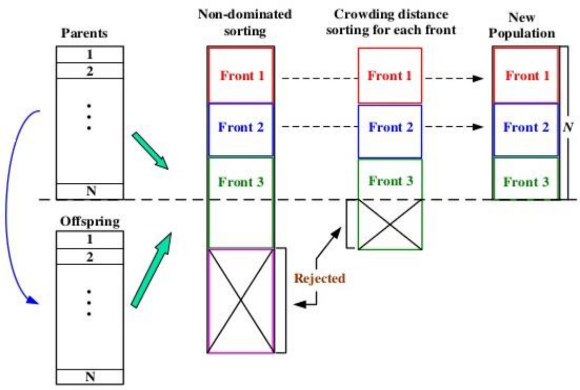

Figure 2. Non-dominated and crowding distance sorting.

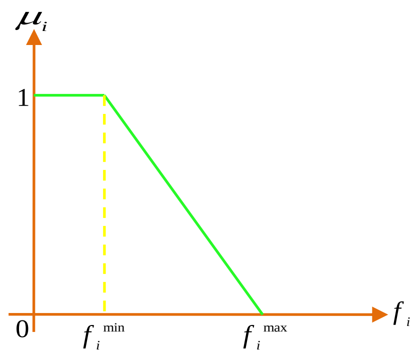

Figure 3. Membership function.

4.5. Pareto-optimal solutions

For a problem with J objectives (o^1, o^2, …, o^J), a solution s = (o_s^1, o_s^2, …, o_s^J) dominates another one s′ = ($o_{s'}^1$, $o_{s'}^2$, …, $o_{s'}^J$) if both of the following conditions are satisfied [21]:

- s is no worse than s' in any attributes

- s is strictly better than s' in at least one attribute.

It can be denoted as $s \succ s'$ or $s' \prec s$. A solution s is defined as covering another one s′ if s is no worse than s' in any attribute. It can be denoted as $s \succcurlyeq s'$ or $s' \preccurlyeq s$.

If a solution s cannot be dominated by another one s', it can be said that s is non-dominated by s'. If a solution s is non-dominated by all the other solutions in a solution set B, it is called the Pareto-optimal solution in B. The set of all the non-dominated solutions of B is called the Pareto-set of B.

5. Applying MHSA in a multi-objective ORPD problem

The proposed strategy to solve ORPD in the multi-objective framework can be stepped as follows:

Step 1: Generate the initial populations. Firstly, set counter $i = 0$, and generate n random harmony, as follows:

$$D = [D_1, D_2, D_3, ..., D_n] \qquad D_i = (d_i^1, d_i^2, ..., d_i^m) \quad (29)$$

where d_i^j is the j^{th} state variable value of the i^{th} harmony population. For each individual (D_i), the objective function values are calculated.

Step 2: The three conflicted fitness functions, namely J_1, J_2, and J_3 should be minimized simultaneously, while satisfying the system constraints.

Step 3: Update the counter $i= i +1$.

Step 4: Store the positions of the solutions that represent the non-dominated vectors.

Step 5: Determine the best global solution for the i^{th} harmony from the non-dominated sort. First, these hypercubes consisting of more than one solution are assigned a fitness value equal to the result of dividing any number $x>1$ by the number of solutions that they contain. Then apply the crowding distance on the fitness values to select the hypercube.

Step 6: Generate a new population of harmonies based on the proposed mutation, local and global operators.

Step 7: Evaluate each solution by the Newton-Raphson power flow analysis method to calculate the power flow and system transmission loss.

Step 8: Update the contents of the repository non-dominated sort together with the geographical representation of the solutions within the hypercube.

Step 9: Update the contents of the repository solutions.

Step 10: If the maximum iteration $iter_{max}$ is satisfied, then the stop optimization process and print final results. Otherwise, go to step 3.

The graphical illustration is shown in figure 4.

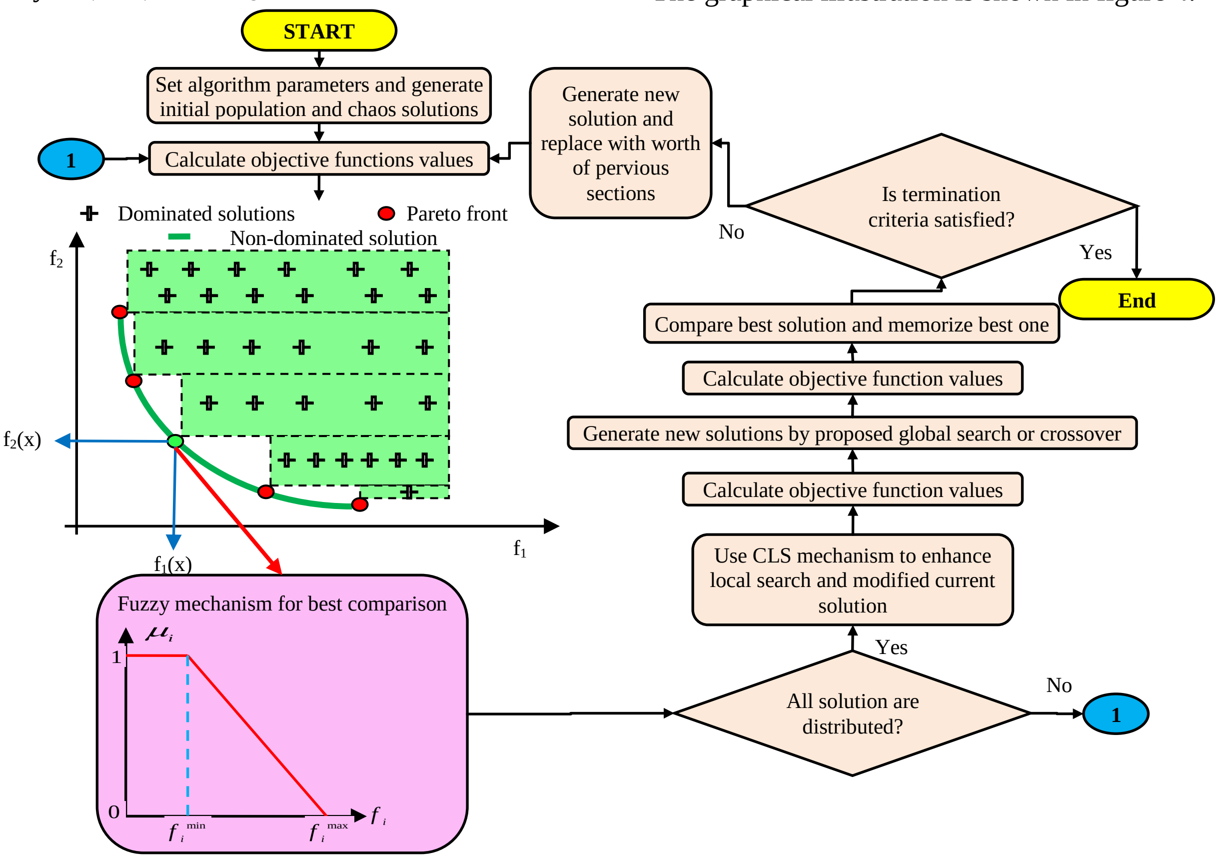

Figure 4. Proposed strategy to solve ORPD problem with modified HAS method.

6. Simulation and discussion

The proposed algorithm was implemented in the MATLAB language 2011a. All simulations were performed on a PC with an Intel Duo Core processor T5800, 2 GHz with a 4GB RAM. In order to access full search ability of the proposed algorithm, test it on the several benchmarks and look at the other articles. As a result, PAR_{min}, PAR_{max}, bw_{min}, and bw_{max} were set with the 0.35, 0.99, 5×10-4, and 0.05 values, respectively. HMCR and HMS were 0.95 and 4, respectively. Also the maximum number of iterations was equal to 500.

6.1. Deterministic model on IEEE 14-bus

At first, the IEEE 14-bus test system was considered with five generator buses (bus 1 was the slack bus, and buses 2, 3, 6, and 8 were PV buses with continuous operating values), 9 load buses and 20 branches, in which 3 branches (4-7, 4-9, and 5-6) were tap changing transformers. Moreover, the candidate buses for shunt compensation were 9 and 14.

Table 1. Results of multi-objective optimization in IEEE 14-bus test system.

Parameters	Case 1		Case 2	
	MHSA	HSA	MHSA	HSA
Vg_2	1.012	1.034	1.132	1.098
Vg_3	1.031	1.065	1.074	1.109
Vg_6	1.029	1.095	1.030	1.165
Vg_8	1.065	1.082	1.072	1.163
$T_{4\text{-}7}$	1.012	1.034	1.028	1.064
$T_{4\text{-}9}$	0.970	0.976	0.907	1.006
$T_{5\text{-}6}$	0.952	0.897	0.989	0.943
Qc_9	0.324	0.302	0.302	0.325
Qc_{14}	0.058	0.047	0.073	0.049
J_1	**1.176**	**1.209**	**1.175**	**1.206**
J_2	**0.205**	**0.243**	0.298	0.652
J_3	0.137	0.135	**0.113**	**0.120**
Parameters	**Case 3**		**Case 4**	
	MHSA	**HSA**	**MHSA**	**HSA**
Vg_2	1.093	1.103	1.083	1.053
Vg_3	1.065	1.095	1.094	1.064
Vg_6	1.083	1.163	1.028	1.093
Vg_8	1.001	1.154	1.014	1.172
$T_{4\text{-}7}$	1.039	1.196	1.004	1.106
$T_{4\text{-}9}$	1.042	0.895	1.042	0.953
$T_{5\text{-}6}$	0.987	0.854	0.987	0.803
Qc_9	0.393	0.473	0.386	0.401
Qc_{14}	0.063	0.035	0.057	0.038
J_1	1.195	1.268	**1.177**	**1.210**
J_2	**0.203**	**0.438**	**0.208**	**0.448**
J_3	**0.114**	**0.123**	**0.115**	**0.125**

In order to evaluate the effectiveness of the proposed algorithm in this test system, four different cases were considered as follow:

Case 1: Consider two objective functions; real power loss (J_1) and voltage deviation (J_2).

Case 2: Consider two objective functions; real power loss (J_1) and voltage stability index (J_3).

Case 3: Consider two objective functions; voltage deviation (J_2) and voltage stability index (J_3).

Case 4: Consider all objective functions; J_1, J_2, and J_3.

The numerical results of these case studies with 9 variables were tabulated in table 1, satisfying the system constrains. In all cases, the lower and upper limits of reactive powers were 0-30 MVAr, and these limits for the transformer tap settings and voltage magnitude were considered within the interval 0.9-1.1 p.u, respectively. The simulation results for the algorithms are shown in table 2. It can be seen that the results obtained for MHSA are better than those for the standard HSA algorithm in all cases. The Pareto front of the proposed algorithm for all cases is shown in figure 5.

Moreover, in order to show the robustness of the proposed algorithm to solve the ORPD problem, consider all objective functions, and optimize them by 30 trails that were individually run for 30 times. The simulation results of these trails are given in figure 6.

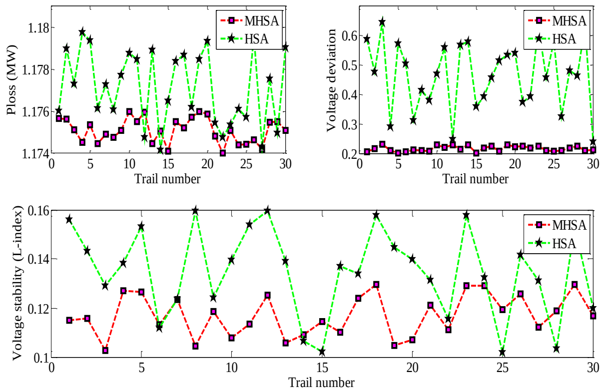

Figure 6. Distribution of final results for proposed algorithm in 30 trials, which simultaneously optimize three objective functions.

It is clear that the variation range of the best total cost during 30 trails simulations is small, which indicates that the MHSA algorithm is stable compared to HSA.

6.2. Deterministic model on IEEE 30-bus

The proposed algorithm was carried out on the IEEE 30-bus test system, which consisted of six thermal plants, 26 buses, and 46 transmission lines. The other useful line data and bus data were taken from [7]. Moreover, it had four transformers, with the off-nominal tap ratio at lines 6–9, 6–10, 4–12, and 28–27. In addition, buses 10, 12, 15, 17, 20, 21, 23, 24, and 29 were selected as shunt VAR compensation buses.

The results of the proposed algorithm were compared with SGA, PSO, GSA, standard HAS, etc, all of which were referred to [7] and [18]. The load of system was P_{load} = *2.832* p.u and Q_{load} =

1.262 p.u on a 100 MVA base. In this case, the optimization problem had 19 control variables, which were presented in table 2.

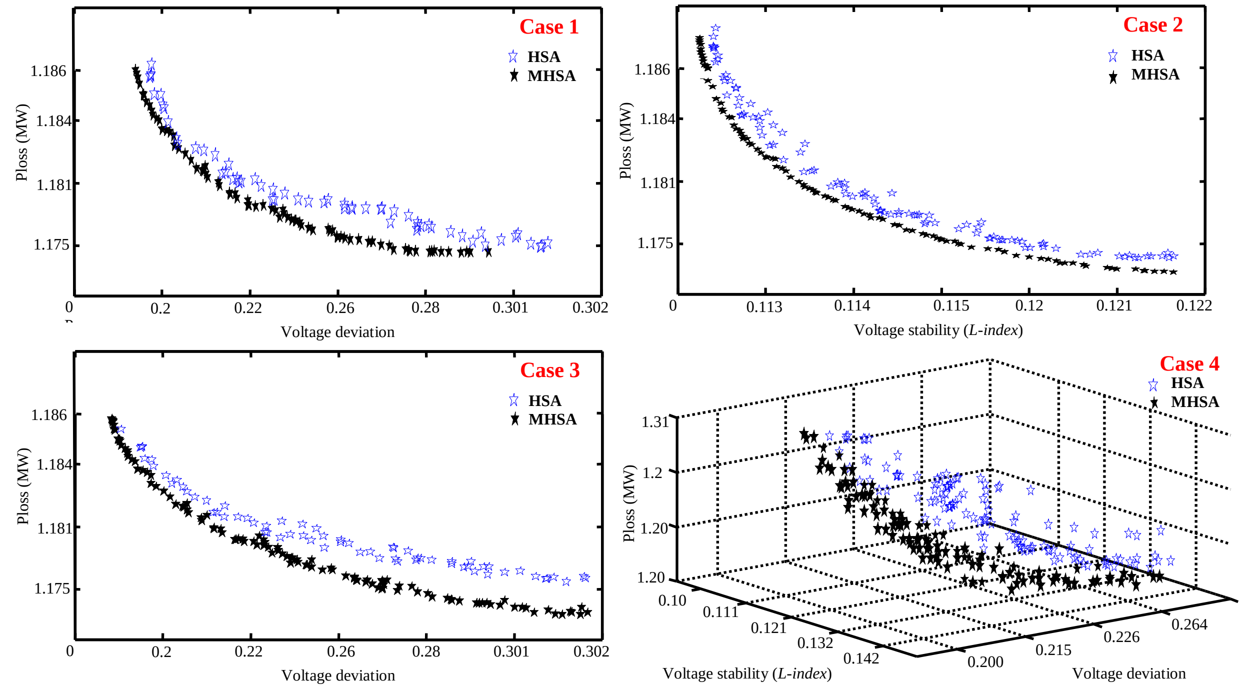

Figure 5. Pareto-optimal front of proposed approach, IEEE 14 bus.

Table 2. Variable limits (p.u.).

Reactive power generation limits							**Voltage and tab setting limits**					
Bus	1	2	5	8	11	13	**Bus**	1	2	5	8	11
Q_G^{max}	0.596	0.48	0.6	0.53	0.15	0.155	V_G^{max}	V_G^{min}	V_{load}^{max}	V_{load}^{min}	T^{max}	T^{min}
Q_G^{min}	-0.298	-0.24	-0.3	-0.265	-0.075	-0.078	1.1	0.9	1.05	0.95	1.05	0.95
				Reactive compensation devices and voltage limits								
				Q_C^{max}	V_G^{max}	V_G^{max}	V_G^{min}					
				0.36	-0.12	1.05	0.95					

Table 3. Comparison of transmission loss for different methods in IEEE 30-bus system.

Algorithm	**GAMs**	**PSO [7]**	**HSA [7]**	**DE [7]**	**SQP [7]**	**GSA [7]**	**BBO [7]**	**BF [18]**
Best Ploss (MW)	4.5468	4.9239	4.9059	5.011	5.043	4.51431	4.5511	4.623
Worst Ploss (MW)	4.8932	5.0576	4.9653	---	---	---	---	4.64
Average Ploss (MW)	5.1029	4.9720	4.9240	---	---	---	---	4.68
CPU time, s	11.82	---	---	---	---	94.6938	---	---
Algorithm	**CPVEIHBMO [7]**	**BF [18]**	**ABC [18]**	**FF [18]**	**HBMO [7]**	**HFA [18]**	**ALC-PSO [18]**	**MHSA**
Best Ploss (MW)	4.37831	4.623	4.6022	4.5691	4.40867	4.529	4.4793	4.373
Worst Ploss (MW)	4.4901	4.64	4.61	4.578	4.8869	4.5325	4.5036	4.487
Average Ploss (MW)	4.4826	4.68	4.63	4.59	4.6453	4.546	4.4874	4.480
CPU time, s	66.038	---	---	---	67.413	---	---	65.02

The simulation results were tabulated in table 3. As it is evident in this table, the proposed method demonstrates its superiority in the ORPD problem, success rate, and solution quality over the other heuristic methods. Moreover, these results confirm the potential of multi-objective MHSA algorithm to solve real-world highly non-linear constrained multi-objective optimization problems. For the sake of a fair comparison, the results obtained by the MHSA algorithm in term of power loss reduction were compared with the other algorithms [7], in which the constraints and initial settings of the problem were different with the assumed values and constraints (four reactive compensation devices were installed at buses 6, 17, 18, and 27). Figure 7 shows a comparison between the different algorithms. The results obtained show that the proposed method demonstrates its superiority in computational complexity, success rate, and solution quality over the PSO, GSA, HSA, HBMO, IPM, and DE methods. For the sake of a fair comparison among the developed methods, 10 independent runs were carried out.

6.3. Deterministic model on IEEE 118-bus

For the completeness and comparison purposes, this is the largest practical test system which we can find in the literature with the complete data required for the ORPD problem. In order to test and validate the robustness of the proposed algorithm, the simulations were carried out in the IEEE 118-bus test system. This network consisted of 186 branches, 54 generator buses, and 12 capacitor banks. Nine branches 8-5, 26-25, 30-17, 38-37, 63-59, 64-61, 65-66, 68-69, and 81-80 were tap changing transformers [19].

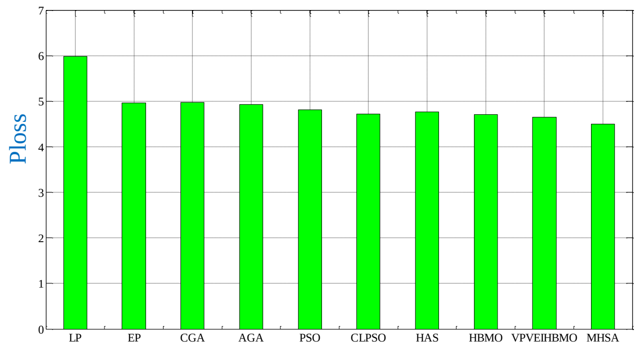

Figure 7. Comparison of proposed method with results exposed in [7].

The capacity of the 12 shunt compensators were within the interval (0, 30) MVAr. All bus voltages were required to be maintained within the range of (0.95, 1.1) p.u. In this regard, consider the following operating condition to compare the performance of the proposed algorithm with the other available methods.

Case 1: To show the effectiveness of the proposed approach, initially, three different objectives namely, transmission loss minimization, voltage profile improvement, and voltage stability index minimization were considered individually. To demonstrate the superiority of the proposed MHSA, the simulation results were compared with the various well-known methods available in the literature, namely, PSO, FIPS, QEA, ACS, DE, SGA, PSO, MAPSO, SOA, TLBO, and QOTLBO. For the convenience of the reader, these methods are collaborated in [20]. The simulation results were tabulated in table 4.

Case 2: In this case study, consider that all the objective functions are simultaneous. The simulation results are given in table 5.

Table 4. Comparison results for IEEE 118-bus system in case 1.

Index	Loss minimization (MW)									
	MHSA	QOTLBO [19]	TLBO [19]	PSO [19]	ALC-PSO [19]	FIPS [19]	QEA [19]	ACS [19]	GAM	DE [19]
Best	111.092	112.2789	116.4003	118.0	121.53	120.6	122.22	131.90	112.142	128.31
Worst	113.72	115.4516	121.3902	122.3	132.99	120.7	NA	NA	113.731	NA
Mean	112.91	113.7693	118.4427	120.6	123.14	120.6	NA	NA	112.642	NA
Standard deviation	0.012	0.0244	0.0482	NA	0.00	NA	NA	NA	0.014	NA

Index	Voltage deviation minimization (p.u.)				L-index minimization			
	MHSA	QOTLBO [19]	TLBO [19]	GAM	MHSA	GAM	QOTLBO [19]	TLBO [19]
Best	0.1864	0.1910	0.2237	0.1875	0.0603	0.0607	0.0608	0.0613
Worst	0.2201	0.2267	0.2543	0.2412	0.0607	0.0608	0.0631	0.0646
Mean	0.1985	0.2043	0.2306	0.1989	0.0608	0.0611	0.0616	0.0626
Standard deviation	0.0342	0.0356	0.0384	0.0403	0.0402	0.0399	0.0476	0.0488

Table 6. Simulation results obtained by MHSA for case 2 in IEEE 118-bus test system.

Control variables	MHSA	Control variables	MHSA	Control variables	MHSA	Control variables	MHSA
Vg1 (p.u.)	1.0166	**Vg49 (p.u.)**	1.008	**Vg90 (p.u.)**	1.0201	**QC48 (p.u.)**	0.0769
Vg4 (p.u.)	0.999	**Vg54 (p.u.)**	1.0215	**Vg91 (p.u.)**	1.009	**QC74 (p.u.)**	0.0970
Vg6 (p.u.)	1.022	**Vg55 (p.u.)**	1.0146	**Vg92 (p.u.)**	1.0048	**QC79 (p.u.)**	0.1091
Vg8 (p.u.)	1.0244	**Vg56 (p.u.)**	1.0136	**Vg99 (p.u.)**	1.0094	**QC82 (p.u.)**	0.0544
Vg10 (p.u.)	1.0172	**Vg59 (p.u.)**	1.024	**Vg100 (p.u.)**	1.0007	**QC83 (p.u.)**	0.1208
Vg12 (p.u.)	1.0194	**Vg61 (p.u.)**	1.0061	**Vg103 (p.u.)**	1.0017	**QC105 (p.u.)**	0.1087
Vg15 (p.u.)	1.019	**Vg62 (p.u.)**	1.0194	**Vg104 (p.u.)**	1.0247	**QC107 (p.u.)**	0.0861
Vg18 (p.u.)	1.0091	**Vg65 (p.u.)**	1.0193	**Vg105 (p.u.)**	1.0251	**QC110 (p.u.)**	0.0821
Vg19 (p.u.)	1.0166	**Vg66 (p.u.)**	1.0088	**Vg107 (p.u.)**	1.0143	**T8-5**	0.9903
Vg24 (p.u.)	1.0028	**Vg69 (p.u.)**	1.0141	**Vg110 (p.u.)**	0.9997	**T26-25**	1.0141
Vg25 (p.u.)	1.018	**Vg70 (p.u.)**	1.0001	**Vg111 (p.u.)**	1.0046	**T30-17**	0.9896
Vg26 (p.u.)	0.9989	**Vg72 (p.u.)**	0.9995	**Vg112 (p.u.)**	1.008	**T38-37**	0.9907
Vg27 (p.u.)	1.0058	**Vg73 (p.u.)**	1.013	**Vg113 (p.u.)**	1.0212	**T63-59**	1.008
Vg31 (p.u.)	0.9993	**Vg74 (p.u.)**	1.0201	**Vg116 (p.u.)**	0.9984	**T64-61**	0.9917
Vg32 (p.u.)	1.0007	**Vg76 (p.u.)**	1.0244	**QC5 (p.u.)**	0.0908	**T65-66**	1.0193
Vg34 (p.u.)	1.0213	**Vg77 (p.u.)**	1.0017	**QC34 (p.u.)**	0.0712	**T68-69**	1.0193
Vg36 (p.u.)	1.0177	**Vg80 (p.u.)**	1.0141	**QC37 (p.u.)**	0.1063	**T81-80**	1.0157
Vg40 (p.u.)	1.007	**Vg85 (p.u.)**	1.0113	**QC44 (p.u.)**	0.0628		
Vg42 (p.u.)	1.0249	**Vg87 (p.u.)**	0.9983	**QC45 (p.u.)**	0.1018		
Vg46 (p.u.)	0.999	**Vg87 (p.u.)**	1.0075	**QC46 (p.u.)**	0.0624		

It is clear that the proposed method yielded better solutions than QOTLBO, the original TLBO, and the other methods. According to table 5, the minimum system loss obtained by the proposed algorithm is 133.82 MW. In other words, it can be seen that the saving with the proposed method in the system loss is 0.4% better than the best solution for QOTLBO. Moreover, voltage deviation and *L-index* obtained using MHSA is better than QOTLBO and the original TLBO methods. To the reader's convenience, Table 6 summaries the ORPD results obtained by MHSA including the transmission loss, voltage deviation, *L-index*, and optimal settings of control variables.

Table 5. Comparison of test results for multi-objectives of IEEE 118-bus system using different methods.

Index	J_1, J_2, and J_3		
	MHSA	QOTLBO	TLBO
Loss (MW)	133.82	134.4059	137.4324
Voltage deviation (p.u.)	0.2102	0.2410	0.2612
L-index (p.u.)	0.0585	0.0619	0.0627

6.4. Stochastic model on IEEE 30-bus

To validate the proposed stochastic model in a single objective formulation, the numerical results were presented on a six-bus and a modified IEEE 30-bus test system. It consisted of 30 buses, 37 transmission lines, 6 generators, 4 under-load tap changing transformers, and 2 fixed shunt reactive capacitive power banks. For the tests, assume that there are three forecasted levels of demand: 1) low demand, 2) average demand, and 3) peak demand. They are known to happen with 25%, 50%, and 25% probabilities, respectively. Other information is given in section 6.2. Comparison to section 6.2 added a new shunt reactive capacitive compensator at bus 24, whose maximum capacity is 40 MVar. The data for the different levels of demand active and reactive is given in table 7.

Table 7. Demand levels for modified IEEE 30-bus system.

Bus	PD [MW]			QD [MVar]		
	Low demand	Average demand	Peak demand	Low demand	Average demand	Peak demand
2	16.28	21.70	27.13	9.53	12.70	15.88
3	1.80	2.40	3.00	0.90	1.20	1.50
4	5.70	7.60	9.50	1.20	1.60	2.00
5	70.65	94.20	117.75	14.25	19.00	23.75
7	17.10	22.80	28.50	8.18	10.90	13.63
8	22.50	30.00	37.50	22.50	30.00	37.50
10	4.35	5.80	7.25	1.50	2.00	2.50
12	8.40	11.20	14.00	5.63	7.50	9.38
14	4.65	6.20	7.75	1.20	1.60	2.00
15	6.15	8.20	10.25	1.88	2.50	3.13
16	2.63	3.50	4.38	1.35	1.80	2.25
17	6.75	9.00	11.25	4.35	5.80	7.25
18	2.40	3.20	4.00	0.68	0.90	1.13
19	7.13	9.50	11.88	2.55	3.40	4.25
20	1.65	2.20	2.75	0.53	0.70	0.88
21	13.13	17.50	21.88	8.40	11.20	14.00
23	2.40	3.20	4.00	1.20	1.60	2.00
24	6.53	8.70	10.88	5.03	6.70	8.38
26	2.63	3.50	4.38	1.73	2.30	2.88
29	1.80	2.40	3.00	0.68	0.90	1.13
30	7.95	10.60	13.25	1.43	1.90	2.38

Table 8 shows the reactive power dispatched for reactive sources and the taps settings under load variable transformers by minimizing the active power losses in each demand level. Table 9 shows the voltage magnitude profile.

At load buses, for the three level demands, the voltages are close to their secure lower limit 0.95. However, by the reactive power injection of the fixed or continuous reactive sources installed in some load buses, the voltages are always not as near their secure lower limits.

Table 8. Solution of stochastic model, IEEE 30-bus system.

Bus	Dispatch of Reactive Sources [MVAr]		
	Low demand	Average demand	Peak demand
2	6.48	21.32	59.99
5	21.09	33.75	40.00
8	21.03	36.04	39.98
11	16.32	22.68	24.00
13	7.98	22.56	23.67
24	4.39	9.01	37.26
Bus	**Tap Settings of Transformers [pu]**		
	Low demand	**Average demand**	**Peak demand**
6-9	0.938	0.937	0.951
6-10	1.087	1.094	1.038
4-12	1.028	1.001	1.014
27-28	0.965	0.973	0.949

Table 9. Voltage profile after optimized-30-bus system.

Bus	Low	Ave	Peak	Bus	Low	Ave	Peak
1	0.992	0.978	1.030	16	0.975	1.011	0.997
2	1.008	1.008	1.027	17	1.009	1.011	0.994
3	0.986	1.004	1.032	18	1.007	1.006	1.040
4	0.973	1.020	1.023	19	1.018	0.973	1.034
5	1.012	1.022	1.037	20	1.014	0.976	1.028
6	0.952	1.008	1.020	21	0.971	0.979	1.038
7	0.994	0.980	1.041	22	1.006	1.027	0.992
8	0.964	0.994	1.033	23	0.999	0.990	1.010
9	1.005	0.991	1.024	24	1.017	0.989	1.007
10	0.971	1.001	1.001	25	0.980	1.015	1.019
11	1.001	1.027	0.997	26	0.976	0.976	1.020
12	0.990	1.013	0.997	27	0.997	1.015	1.033
13	1.002	0.972	1.046	28	1.000	0.990	1.030
14	0.998	1.029	1.030	29	0.959	0.985	1.042
15	1.014	0.984	1.014	30	0.980	1.011	1.018

6.7. Statistical analysis and comparison

In this section, the performance of the multi-objective MHSA is compared with NSGA [21] and MOPSO [22] in Spread (SP) index [23]. This indicator is to measure the extent of spread archived among the non-dominated solutions obtained:

$$SP = \frac{d_f + d_l + \sum_{i=1}^{N-1} |d_i - \bar{d}|}{d_f + d_l + (N-1)\bar{d}} \tag{30}$$

where, N is the number of non-dominated solutions found so far; d_i is the Euclidean distance between neighboring solutions in the obtained non-dominated solutions set, and $\bar{d}$ is the mean of all d_i. The parameters d_f and d_l are the Euclidean distances between the extreme solutions and the boundary solutions of the obtained non-dominated set, respectively. A value of zero for this metric shows that all members of the Pareto optimal set are equidistantly spaced. A smaller value for SP indicates a better distribution and diversity of the non-dominated solutions. Table 10 shows a comparison of the SP metric for different algorithms. It can be seen that the average performance of multi-objective MHSA is much better than the other algorithm results.

Table 10. Comparison of SP-metric for different algorithms.

Index	MHSA	NSGA	MOPSO
Best	0.1683	0.5999	0.2542
Average	0.2789	0.6801	0.3242
Std	0.0089	0.0598	0.0375

7. Conclusion

This paper proposes a modified harmony search algorithm (HSA), which was successfully applied for the ORPD problem solving in deterministic and stochastic models, taking into account the inequality and equality constraints. The ORPD problem was formulated as a multi-objective optimization problem with three conflicted objectives, known as power loss, voltage deviation, and L_{index}. A diversity-preserving mechanism of crowding entropy tactic was investigated to find widely different Pareto optimal solutions. The main contribution of the proposed algorithm can be looked at for the design of local and global search operators and interactive strategy to adjust two significant parameters (i.e. *bw* and *PAR*) during the optimization process, which improves its overall performance. The proposed algorithm was evaluated on the three test systems IEEE 14-bus, 30-bus, and 118-bus to demonstrate its effectiveness compared to other available algorithms. It was seen that the ability of the proposed algorithm to jump out of the local optima, the convergence precision, and speed were enhanced remarkably. Furthermore, the results obtained showed the capabilities of the proposed algorithm to generate well-distributed Pareto solutions. Moreover, the uncertainty in generating units in the form of system contingencies was considered in the reactive power optimization procedure by the stochastic model. Hereby, it is expected that the proposed MHSA algorithm is preferred, and it plays a more active role in the reactive power dispatch problem.

References

[1] Ghasemi, A., Golkar, M. J., Golkar, A.& Eslami, M. (2016). Reactive power planning using a new hybrid technique. Soft Comput, vol. 20, pp. 589-605.

[2] Mehdinejad, M., Mohammadi-Ivatloo, B., Dadashzadeh-Bonab, R.& Zare, K. (2016). Solution of optimal reactive power dispatch of power systems using hybrid particle swarm optimization and imperialist competitive algorithms. Int. J. Electr. Power Energy Syst. vol. 83, pp. 104-116.

[3] Kirschen, D. S. & Van Meeteren, H. P. (1988). MW/voltage control in linear programming based optimal power flow. IEEE Trans. Power Syst. vol. 3, pp. 481-489.

[4] Lee, K. Y., Park, Y. M. & Ortiz., J. L. (1985). A united approach to optimal real and reactive power dispatch. IEEE Trans. Power Apparatus Syst. vol. 104, pp. 1147-1153.

[5] Nanda, J., Kothari, D. P. & Srivastava, S. C. (1989). New optimal power dispatch algorithm using Fletcher's quadratic programming method. IEE Electr. Power Gener. Transm. Distrib. vol. 136, pp. 53-161.

[6] Momeh, JA., Guo, SX., Oghuobiri, EC. & Adapa, R. (1994). The quadratic interior point method solving the power system optimization problems. IEEE Trans Power Syst, vol. 9, no. 3, pp. 1327-1336.

[7] Ghasemi, A., Valipour, K. & Tohidi, A. (2014). Multi objective optimal reactive power dispatch using a

new multi objective strategy. Int. J. Electr. Power Energy Syst., vol. 57, pp.318-334.

[8] Basu, M. (2016). Quasi-oppositional differential evolution for optimal reactive power dispatch. Int. J. Electr. Power Energy Syst., vol. 78, pp. 29-40.

[9] Basu, M. (2016). Multi objective optimal reactive power dispatch using multi objective differential evolution. Int. J. Electr. Power Energy Syst., vol. 82, pp. 213-224.

[10] Biswas (Raha), S., Mandal, K. K. & Chakraborty, N. (2016). Pareto-efficient double auction power transactions for economic reactive power dispatch. Applied Energy, vol. 168, pp. 610-627.

[11] Sulaiman, M. H., Mustaffa, Z., Mohamed, M. R. & Aliman, O. (2015). Using the gray wolf optimizer for solving optimal reactive power dispatch problem. Applied Soft Computing, vol. 32, pp. 286-292.

[12] Geem, Z. W., Kim, J. H. & Loganathan, G. V. (2011). A new heuristic optimization algorithm: harmony search. Simulation, vol. 76, no. 2, pp. 60-68.

[13] Kazemi, A., Parizad, A. & Baghaee, H. R. (2009). On the use of harmony search algorithm in optimal placement of facts devices to improve power system security. in: Proceedings of EUROCON, pp. 570-576.

[14] Dash, R. & Dash, P. (2016). Efficient stock price prediction using a Self Evolving Recurrent Neuro-Fuzzy Inference System optimized through a Modified Differential Harmony Search Technique. Expert Systems with Applications, vol. 52, pp. 75-90.

[15] Pandiarajan, K. & Babulal, C. K. (2016). Fuzzy harmony search algorithm based optimal power flow for power system security enhancement. Int. J. Electr. Power Energy Syst., vol. 78, pp. 72-79.

[16] Hu, Z., Wang, X. & Taylor, G. (2010). Stochastic optimal reactive power dispatch: Formulation and solution method. Electr. Power Energy Syst., vol. 32, pp. 615-621.

[17] Ghasemi, A., Gheydi, M., Golkar, M. J. & Eslami, M. (2016). Modeling of Wind/Environment/Economic Dispatch in power system and solving via an online learning meta-heuristic method. Applied Soft Computing, vol. 43, pp. 454-468.

[18] Rajan, A. & Malakar, T. (2015). Optimal reactive power dispatch using hybrid Nelder–Mead simplex based firefly algorithm. Electrical Power and Energy Systems, vol. 66, pp. 9-24.

[19] Power systems test case archive, http://www.ee.washington.edu/research/pstca.

[20] Mandal, B. & Roy, P. K. (2013). Optimal reactive power dispatch using quasi-oppositional teaching learning based optimization. Electrical Power and Energy Systems, vol. 53, pp. 123-134.

[21] Mosavi, A. (2014). Data mining for decision making in engineering optimal design. Journal of AI and Data Mining, vol. 2, no. 1, pp. 7-14.

[22] Shayeghi, H. & Ghasemi, A. (2012). Economic Load Dispatch Solution Using Improved Time Variant MOPSO Algorithm Considering Generator Constraints. International Review of Electrical Engineering, vol. 7, no. 2, pp. 4292-4303.

[23] Deb, K., Pratap, A., Agarwal, S. & Meyarivan, T. (2002). A fast and elitist multiobjective genetic algorithm: NSGA-II. IEEE Trans. Evol. Comput., vol. 6, no. 2, pp. 182-19.

[24] Zitzler, E., Deb, K. & Thiele, L. (2000). Comparison of multiobjective evolutionary algorithms: empirical results. Evol. Comput. J. vol. 8, pp. 125-148.

نشریه هوش مصنوعی و داده کاوی

بکارگیری یک مدل بهبود یافته الگوریتم جستجوی هارمونی برای مساله چند هدفه توزیع توان راکتیو برای مدل‌های قطعی و غیر قطعی

خلیل ولیپور* و علی قاسمی

دانشگاه محقق اردبیلی، دانشکده فنی مهندسی، گروه برق قدرت، اردبیل، ایران.

ارسال ۲۰۱۶/۰۱/۱۲؛ پذیرش ۲۰۱۶/۰۵/۳۰

چکیده:

توزیع بهینه توان راکتیو یکی از مسائل مهم در برنامه‌ریزی سیستم قدرت بوده که با وجود متغیرهای گسسته و پیوسته دارای قیود غیرخطی و توابع هزینه ناصاف می‌باشد. در این مقاله ابتدا به مدلسازی مساله توزیع توان راکتیو در دو مدل قطعی و غیرقطعی پرداخته شده است. در مدل قطعی از سه تابع تلفات، پایداری ولتاژ و پایداری L به صورت چند هدفه برای حل آن استفاده شده است. در مدل غیرقطعی براساس توابع امید ریاضی و احتمالات به مدلسازی تابع تلفات پرداخته شده است که در نهایت این تابع هدف مورد کمینه‌سازی قرار می‌گیرد. از آنجایی که این مساله پیچیده می‌باشد از یک الگوریتم بهبودیافته جستجوی هارمونی به صورت چندهدفه و تک‌هدفه به حل آن پرداخته شده است. روش پیشنهادی بر روی سیستم‌های تست مختلف اعمال و نتایج حاصله با سایر روش‌های موجود مورد بحث و بررسی قرار گرفته است. نتایج نشان از کارایی بالای الگوریتم پیشنهادی در حل مساله چندهدفه توان راکتیو دارد.

کلمات کلیدی: توزیع توان راکتیو، الگوریتم بهبودیافته جستجوی هارمونی، مدلسازی چندهدفه، پایداری سیستم، مدل غیرقطعی.